

LATE AGB MAGNETIC CYCLES: MHD SOLUTIONS FOR THE HST PN RINGS

Guillermo García-Segura¹, José Alberto López², José Franco^{3,4}

Instituto de Astronomía-UNAM, Apdo Postal 877, Ensenada, 22830 Baja California,
Mexico

Received _____; accepted _____

¹Email address: ggs@astrosen.unam.mx

²Email address: jal@astrosen.unam.mx

³Instituto de Astronomía-UNAM, Apdo Postal 70-264, 04510 México D. F., Mexico

⁴Email address: pepe@astroscu.unam.mx

ABSTRACT

The Hubble Space Telescope has revealed the existence of multiple, regularly spaced, and faint concentric shells around some planetary nebulae. Here we present 2(1/2)D magnetohydrodynamic numerical simulations of the effects of a solar-like magnetic cycle, with periodic polarity inversions, in the slow wind of an AGB star. The stellar wind is modeled with a steady mass-loss at constant velocity. This simple version of a solar-like cycle, without mass-loss variations, is able to reproduce many properties of the observed concentric rings. The shells are formed by pressure oscillations, which drive compressions in the magnetized wind. These pressure oscillations are due to periodic variations in the field intensity. The periodicity of the shells, then, is simply a half of the magnetic cycle, because each shell is formed when the magnetic pressure goes to zero during the polarity inversion. As a consequence of the steady mass-loss rate, the density of the shells scales as r^{-2} , and their surface brightness has a steeper drop-off, as observed in the shells of NGC 6543, the best documented case of these HST rings. Deviations from sphericity can be generated by changing the strength of the magnetic field. For sufficiently strong fields, a series of symmetric and equidistant blobs are formed at the polar axis, resembling the ones observed in He 2-90. These blobs are originated by magnetic collimation within the expanding AGB wind.

Subject headings: Hydrodynamics—ISM: Planetary Nebulae, jets and outflows, bubbles, —ISM: Individual (NGC 6543, Hb 5, He 2-90 , K 1-2)—Stars: AGB

1. Introduction

The multiple concentric rings, or arcs, that were recently discovered by the Hubble Space Telescope around a handful of planetary nebulae (PNe) (see Kwok, Su, & Hrivnak 1998; Terzian & Hajian, 2000 and references therein) is one of the most puzzling and unexpected results delivered by the HST. The best documented case of these systems of faint concentric rings (hereafter called HST rings) is displayed by NGC 6543 (Balick, Wilson & Hajian 2000). In reality, they are regularly spaced concentric shells, indicating quasi-periodic events with time intervals, assuming typical expansion velocities of AGB winds, in the range of 500 to 1500 years. These time scales are too short for thermal pulses and too long for acoustic envelope pulsations. Thus, the origin of the rings cannot be ascribed to any of this type of events. Soker (2000) made a critical review of the mechanisms that have been proposed to explain them, and he indicates that mass-loss variations associated with solar-like magnetic cycles are perhaps the best alternative for their origin. In his view, the magnetic field plays no direct role in the evolution of the AGB wind but the variation in the number of magnetic spots is able to modify the mass-loss rate. The number of cool spots over the AGB surface, which could be preferred sites for dust formation, is controlled by the magnetic cycle. Thus, given that the mass-loss is driven by radiation pressure on dust grains, the same cycle may also regulate periodic variations in the mass-loss rate. In this interpretation, the magnetic field is a passive player with no dynamical effects, and the mass-loss rate simply follows the spot cycle activity. In addition, to make a logical association with bipolar PNe, he suggests that a stronger magnetic activity could be expected from dynamo amplification in binary systems.

Here we develop a different point of view and explore some of the actual dynamical effects of a solar-like magnetic cycle. We build a very simple model, without mass-loss variations, and perform 2(1/2)D magnetohydrodynamic computations considering a cyclic

polarity inversion of the surface magnetic field of an AGB star. Our results show the importance of MHD effects in the formation of the HST rings and successfully reproduce their main features. This indicates that modulated mass-loss episodes are not really necessary to generate the rings. In Section 2 we describe the MHD models and results. A brief discussion is given in Section 3.

2. Numerical Models

2.1. The Method

The simulations have been performed using the magnetohydrodynamic code ZEUS-3D (version 3.4), developed by M. L. Norman and the Laboratory for Computational Astrophysics. This is a finite-difference, fully explicit, Eulerian code descended from the code described in Stone & Norman (1992). A method of characteristics is used to compute magnetic fields, as described in Clarke (1996), and flux freezing is assumed in all the runs. We have used spherical polar coordinates (r, θ, Φ) , with reflecting boundary conditions at the equator and the polar axis. Rotational symmetry is assumed with respect to the rotational (polar) axis, and our models are effectively two-dimensional. The simulations are carried out in the meridional (r, θ) plane, but three independent components of the velocity and magnetic field are computed (*i. e.*, the simulations are “two and a half” dimensions).

Our grids consist of 200×180 equidistant zones in r and θ , respectively (with a radial extent of 0.1 pc, and an angular extent of 90°), and the innermost radial zone lies at $r = 2.5 \times 10^{-3}$ pc from the central star. These values are used in all the simulations shown in Figures 1 – 3.

The equations for the stellar wind flow are simple, since we model an isothermal, slow AGB wind with constant mass-loss rate ($10^{-6} M_\odot \text{ yr}^{-1}$) and radial velocity (10 km s^{-1}).

These values represent the boundary conditions used in the first five innermost radial zones. Rotational effects are not important in these outflows, since we have used a small value for the stellar rotation velocity, 0.01 km s^{-1} (see García-Segura et al. 1999 for more details).

The novel aspect in this letter is the simple treatment of the stellar magnetic field (B_s), which it is allowed to change sign in a cycle of the form:

$$B_s(t) = B_{\max} \cos(2\pi \frac{t}{P}), \quad (1)$$

where B_{\max} is the maximum average B-field at the AGB surface, and P is the period of the magnetic cycle. Since we do not know the true variation form of the field, this functional form is just a first simple approximation. The equation for the wind toroidal field, then, is:

$$B_\phi(t) = B_s(t) \frac{v_{\text{rot}}}{v_\infty} \left(\frac{R_s}{r} \right)^2 \left(\frac{r}{R_s} - 1 \right) \sin\theta, \quad (2)$$

where v_{rot} is the stellar rotation velocity, v_∞ the wind velocity, and R_s the stellar radius. The function $\sin\theta$ cancels the toroidal component at the symmetry (polar) axis. The poloidal field component can be neglected at large distances, so that our field configuration naturally satisfies the condition $\nabla \cdot B = 0$.

The parameter which identifies our models is the ratio of the magnetic field energy density to the kinetic energy density in the wind (Begelman & Li 1992)

$$\sigma(t) = \frac{B^2}{4\pi\rho v_\infty^2} = \frac{B_s^2(t) R_s^2}{\dot{M} v_\infty} \left(\frac{v_{\text{rot}}}{v_\infty} \right)^2. \quad (3)$$

Obviously, this parameter is always positive and oscillates with twice the frequency of the stellar magnetic cycle.

2.2. Results

The first model, shown in Figure 1, corresponds to the case of a slow and dense wind ($v_\infty = 10 \text{ km s}^{-1}$ and $\dot{M} = 10^{-6} M_\odot \text{ yr}^{-1}$), in which the magnetic field at the surface of

the AGB star cycles with a full period of 2000 yr. A peak value $\sigma_{\max} = 0.01$ is used for a slowly rotating AGB star ($v_{\text{rot}} = 0.01 \text{ km s}^{-1}$), which is achieved, for example, when the star has $B_s = 53 \text{ G}$ and $R_s = 1 \text{ AU}$, or $B_s = 113 \text{ G}$ and $R_s = 100 \text{ R}_\odot$. For the cases discussed by Soker (2000), $R_s = 2 \text{ AU}$ and $0.2 \text{ km s}^{-1} \leq v_{\text{rot}} \leq 2 \text{ km s}^{-1}$, the required surface magnetic fields are within $1.3 \text{ G} \geq B_s \geq 0.13 \text{ G}$.

Figure 1 displays radial cuts, on the equatorial plane, of some of the wind variables at $t = 10,000 \text{ yr}$ after the onset of the magnetized wind. The first (top) panel shows the existence of equidistant concentric shells, separated by 1,000 yr, a half of the magnetic cycle period. Each density peak corresponds to a minimum in the magnetic pressure (second panel), which also occurs at the moment when the magnetic field changes polarity (fourth panel). The last panel of Figure 1 displays the radial velocity, which clearly shows the gas response to the local variations in the total pressure (third panel) of the wind.

Thus, shell formation in a magnetized wind with variable field strength is a straightforward process. The outflowing plasma notices the magnetic pressure depressions, both upstream and downstream in the wind, and moves towards the low-pressure sites. The wind is then compressed at these locations, increasing the local density, to compensate for the low magnetic pressure values. Obviously, the particular values achieved at these density peaks, and the density contrast between ring and inter-ring zones, depend on the model assumptions. Thus, these values can be modified by changing the amplitude of the pressure fluctuations (*i. e.*, by changing the maximum field intensities, or adding mass-loss or velocity variations, etc.) but, for our purposes, it is sufficient to show that a reasonable density contrast is achieved by this simple model. The total pressure plot (third panel), shows that the local pressure fluctuations decrease with time (or position in the wind). As the plasma flows from the positions of the magnetic peaks and compresses the gas of the valleys, a series of MHD waves are continuously driven that maintains small gas oscillations

in the expanding wind.

Figure 2 shows the emission measure of four different models, with $\sigma_{\max} = 0.001, 0.01, 0.05, 0.1$. The plots nicely reproduce the typical spacing of the rings, and show a general drop-off that scales as r^{-4} , as expected for a constant mass-loss wind with $\rho \sim r^{-2}$. The structures are in reality a set of spherical or quasi-spherical shells, and their projected maximum column densities in the plane of the sky give the impression of concentric rings. For large enough values of σ_{\max} , the magnetized AGB wind is able to self-collimate towards the polar axis. This self-collimation is also present in the free, streaming fast winds that form some PNe (see García-Segura et al. 1999) but, given the large densities of the slow AGB winds, the self-collimated structures are particularly prominent, and easily observable features in this case. The two right panels in Figure 2 clearly show the resulting structures, that are better defined and more conspicuous in the $\sigma_{\max} = 0.1$ case. The self-collimated gaseous structures also follow the periodic variations of the magnetic field, resulting in two strings of regularly spaced blobs located along the polar axis resembling those observed in He 2-90 (Sahai & Nyman 2000).

3. Discussion and Summary

A relevant point for the applicability of this model is whether or not the B -field of an AGB wind can be considered frozen into the outflowing gas, and if the simple MHD effects that we have described are truly operative during wind evolution. This question has been previously explored by several authors and in much more restrictive environments. For instance, in collapsing molecular clouds with ionization fractions as low as 10^{-7} , where ion drift could lead to substantial magnetic flux leakage. Nonetheless, even at these very low ionization fraction values, numerical models of cloud collapse show that the field remains nearly frozen into the cloud for long periods of time (*e. g.* Black & Scott 1982). For AGB

winds the situation is certainly more favorable because the ions are provided by a number of species with low ionization potentials (Habing 1996; Cox 1997), and charged dust grains are also important in coupling the magnetic field to the outflow. Thus, flux leakage is not considered important during the AGB phase, with time scales of the order of 10^3 to 10^5 yr (for cases where ambipolar diffusion is important see Mac Low et al. 1995 and references therein). Later on, the AGB wind is photoionized by the central star of the PN (as in NGC 6543 or Hb 5), and the temperature and ionization fraction of the outflowing plasma is suddenly increased. Some pressure readjustments occur within the photoionized plasma at this time, but the basic shell structuring remains unchanged. Obviously, flux leakage becomes irrelevant after this moment, and the rings can survive for longer periods of time.

Another related question is if the shells can be formed only by modulated mass-loss rate episodes, without magnetic pressure in the wind, as proposed by Soker (2000). In this case, the periodic increase of density in the wind is only due to the increase in mass-loss, and the higher densities can be maintained as long as the wind temperature decreases in these same locations. This is a perfectly reasonable possibility during the AGB phase. However, once the wind becomes photoionized, the plasma temperature becomes fairly homogeneous ,and the rings tend to be washed away in a sound crossing time. Thus, ring survival is severely compromised in the purely hydrodynamic case.

There is one additional feature that suggests that the magnetohydrodynamic case is indeed more important. Recent HST observations of He 2-90 show a series of bright knots which have been interpreted as due to well collimated, symmetric jets (Sahai & Nyman 2000). Up to now, however, there is not kinematic information to conclude that this linear, knotty structure is really a supersonic, fast jet. The similarity of the observed knotty structure with the largest σ_{\max} model presented here provide an attractive, alternative explanation. Figure 3 shows a qualitative comparison of one of the models ($\sigma = 0.1$) with

the structuring of the “jets” in He 2-90 (figure 3 in Sahai & Nyman 2000). As stated above, the peak densities depend on model assumptions and despite the fact that we have not attempted to specifically reproduce this nebula, the similarity is impressive. Thus, although the imaging actually shows something that resembles a jet, our models indicate that this feature could be something very different. If this is the case, the velocity of the observed knots should be the same as the rest of the AGB wind. Another example where slow, or stationary jet-like features have been observed, is K 1-2 (see additional examples in the list discussed by Gonçalves et al. 2001), which may probably be explained by the same mechanism.

The interpretation of Sahai & Nyman has a certain link with our results, since jets are also formed by magnetic collimation. The only difference is that the gas in our case is only collimated but not accelerated. The collimation of the outflow is solely due to the hoop stress of the toroidal field but the acceleration requires an additional process. For instance, the acceleration of a jet-like flow in some planetaries is achieved after the wind passes through a reverse shock and is subsequently pinched at polar axis (Różyczka & Franco 1996). The case of He 2-90 is probably different since, although magnetic collimation is present, there is no acceleration mechanism to create a “supersonic fast jet”. Note that collimation without acceleration can occur in a freely outflowing wind.

In summary, the dynamical effects of a solar-like magnetic cycle operating in late AGB stars have been explored with MHD models. Although a number of simplifying assumptions have been made, the numerical simulations are able to successfully reproduce for the first time the main observed properties of the HST rings. Further studies with less restrictive assumptions may shed more light on the range of MHD effects that may operate in these type of objects.

Acknowledgments It is a pleasure to thank Yervant Terzian for his helpful discussions

and encouragement about this topic during his visit to Ensenada. We also thank Michael L. Norman and the Laboratory for Computational Astrophysics for the use of ZEUS-3D. The computations were performed at Instituto de Astronomía-UNAM. This work has been supported by grants from DGAPA-UNAM (IN130698 and IN117799) and CONACyT (32214-E).

List of References

Balick, B., Wilson, J. & Hajian, A. R. 2000, AJ, 121, 354

Begelman, M. & Li, Z. Y. 1992, ApJ, 397, 187

Black, D. C. & Scott, E. H. 1982, ApJ, 263, 696

Clarke, D. A. 1996, ApJ, 457, 291

Cox, P. 1997, in IAU Symp. No 180 “Planetary Nebulae”, eds. H. J. Habing & H. J. G. L. M. Lamers, (Kluwer Academic Publishers, Dordrecht), 139

Habing, H. J. 1996, A&A Rev., 7, 97

García-Segura, G., Langer, N., Różyczka, M., & Franco, J. 1999, ApJ, 517, 767

Gonçalves, D., Corradi, R. L. M., Mampaso, A. 2001, ApJ, 547, 302

Gonçalves, D., Corradi, R. L. M., Mampaso, A. 2001, in “Emission Lines from Jet Flows”, W. Henney, W. Steffen, L. Binette & A. Raga eds, RMxAASC, in press (astro-ph/0102009)

Kwok, S., Su, K. Y. L., Hrivnak, B. J. 1998, ApJ, 501, L117

Mac Low, M.-M., Norman, M. L., Konigl, A., & Wardle, M. 1995, ApJ, 442, 726

Różyczka, M. & Franco, J. 1996, ApJL, 469, L127

Sahai, R., & Nyman, L.-A. 2000, ApJ, 538, L145

Soker, N. 2000, ApJ, 540, 436

Stone, J. M. & Norman, M. L. 1992, ApJS, 80, 753

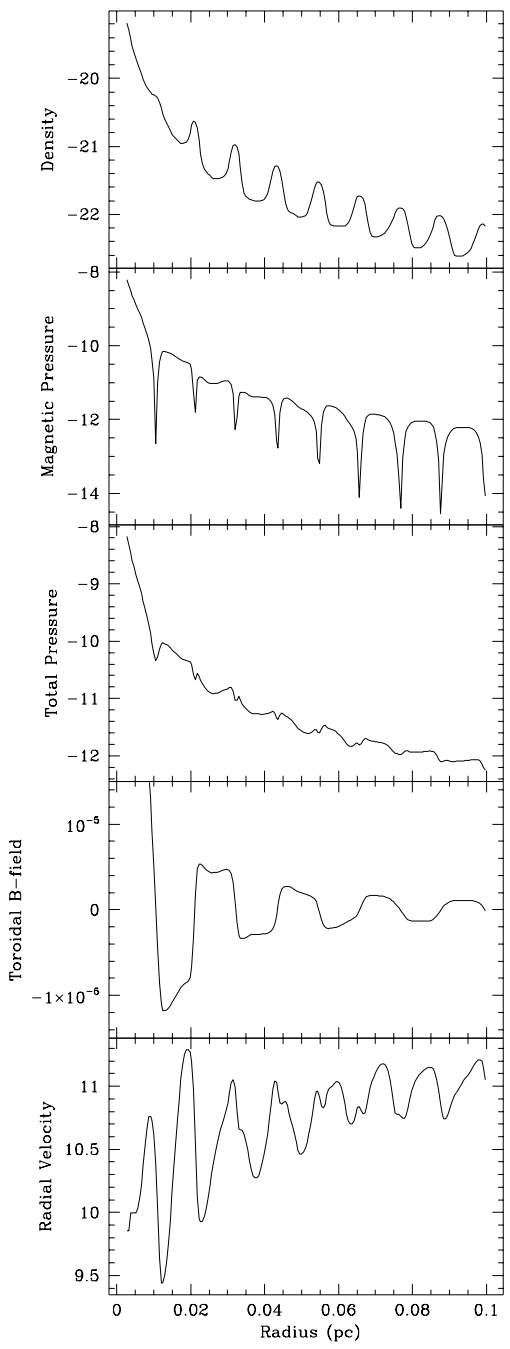
Terzian, Y., & Hajian, A. R. 2000, *Asymmetrical Planetary Nebulae II: From Origins to Microstructures*, eds. Joel H. Kastner, Noam Soker, Saul A. Rappaport, A.S.P. Conference Series, 199, 33

Figure Captions

Figure 1. Equatorial cut for the run with $\sigma = 0.01$ showing the effects of a cyclic polarity inversion of the AGB stellar magnetic field. Each density peak correspond to 1,000 yr, half of the full period. Units are in c.g.s., except for the radial velocity (km s^{-1}).

Figure 2. Emission measure of four different runs projected with a tilt of 45° from the plane of the sky. The panels correspond to: (top-left) $\sigma = 0.001$, (bottom-left) $\sigma = 0.01$, (top-right) $\sigma = 0.05$, (bottom-right) $\sigma = 0.1$. Each concentric shell correspond to 1,000 yr. Note the piled-up blobs at the polar axis for the most magnetized runs, resulting from the self-collimation of the AGB wind.

Figure 3. Comparison between the polar region of the model with $\sigma = 0.1$ (projected without tilt on the plane of the sky) (top), with figure 3 by Sahai & Nyman (2000) of He 2-90 (bottom). In their figure, the relative intensity of the jet is plotted as a function of radius showing the radial offsets of the knots from the center (thick curve: southeast jet, thin curve: northwest jet).



This figure "Figure2.jpg" is available in "jpg" format from:

<http://arxiv.org/ps/astro-ph/0104154v1>

